Effect of sintering conditions on resistivity and dielectric properties of Ni–Zn ferrites

B. PARVATHEESWARA RAO, K. H. RAO
Department of Physics, Andhra University, Visakhapatnam-530 003, India

Resistivity and dielectric properties of the nickel-zinc ferrite composition, $Ni_{0.65}Zn_{0.35}Fe_2O_4$, have been studied near different sintering conditions to optimize the sintering schedule for a specific application. Variable sintering parameters in the study include sintering temperature in the range from 1150 to 1300 °C and sintering time with 1 h, 2 h and 4 h durations at each sintering temperature. The results indicate that the decrease of resistivity is linear and less rapid upto a sintering schedule of 1250 °C/2 h, and thereafter any increase either in sintering temperature or in sintering time causes a rapid decrease of resistivity due to the increased volatilization of zinc from the samples at these temperatures/times. Possible mechanisms contributing to conduction processes in ferrites are discussed in explaining the obtained results.

1. Introduction

The importance of soft magnetic ferrites, particularly nickel–zinc and manganese–zinc ferrites, in the transformer and telecommunication fields is well known and their uses in these fields have been continuously increasing for several decades. For this reason, the electrical and magnetic properties of these materials have been investigated by a number of researchers. Many of these properties are highly dependent on processing parameters such as sintering temperature, sintering time, and heating atmosphere etc., as these parameters greatly influence crystal composition and size, and also the size and volume of pores.

The electrical properties of nickel–zinc ferrites with respect to sintering conditions were reported by many workers. However, the results of different investigators [1–5] are often conflicting. Van Uitert [1] reported that the room temperature resistivity of nickel–zinc ferrites increased with increase of firing temperature for a fixed sintering time because of improved homogenization and structural perfection. A similar reasoning was given by Secrist and Turk [2] for the observed increase in resistivity in Ni–Zn ferrite system, with increase in sintering time for the sintering temperatures $\geqslant 1170$ °C. They reported that the resistivity was same for the samples fired either in air or in oxygen atmospheres, and further concluded that the resistivity was independent of grain size between 6.3 and 14.8 μm.

In contrast, Naik and Power [3] have found a reduction both in resistivity and in activation energy for the Ni–Zn ferrites when sintered at higher temperature. The observed decrease has been attributed to the reduced porosity and increased grain size at the higher sintering temperature. Jain *et al.* [4] have also observed a decrease in d.c. resistivity in vanadium-doped Ni–Zn ferrites with increase of sintering temperature.

Koops [5] subjected a series of nickel–zinc ferrites, all of the same composition but to various sintering conditions and attributed the observed variations in resistivity and dielectric constant to the presence of Fe^{2+} concentration developed in the firing. The variable sintering parameters in this study are temperature, time, atmosphere and cooling schedule; all these parameters are found to be more or less important in determining the electrical properties.

In view of the above, it is felt necessary and important to conduct a systematic study of Ni–Zn ferrites as a function of sintering temperature and sintering time. Variations in resistivity and dielectric constant with respect to sintering conditions are presented in this paper. Variations of resistivity with temperature and applied field, and frequency response of dielectric constant and loss tangent are also discussed.

2. Experimental details

Samples of the composition $Ni_{0.65}Zn_{0.35}Fe_2O_4$ were prepared by taking reagent grade oxides of nickel, zinc and iron powders of greater than 99.5% purity. The initial ingredients were intimately mixed in correct proportions and ground for 5 h using an agate mortar and pestle in the presence of methanol to improve homogeneity. The resulting mixture was air dried and pre-sintered in air for 4 h at 900 °C. The pre-sintered ferrite was again ground for a few hours in the presence of methanol, air dried and granulated by using 5% polyvinyl alcohol as binder. The granulated powder was then pressed into pellets, at a pressure of 100 MPa, which were subsequently sintered in air atmosphere for varying durations of time (1, 2 and 4 h) at each temperature in the range from 1150 to 1300 °C at intervals of 50 °C. After the completion of the sintering period, cooling of the samples was carried out at an approximate rate of 200 °C per hour for 2 h from

0022–2461

the peak temperatures respective, and subsequently the furnace was switched off and the samples were allowed to cool naturally to 60 °C.

X-ray diffraction studies reveal single phase spinel structures for all the samples, and the sample densities were approximately 90–93% of their theoretical limits. Characterization of the samples was done by measuring their Curie temperatures (390 ± 5 °C) which compare favourably with the reported value for the same ferrite composition [6].

D.c. resistivity measurements have been made by the conventional two probe method using spring loaded copper electrodes connected to Keithley model 614 digital electrometer. For temperature variation of resistivity, the cell containing the sample was kept in a furnace and maintained at the desired temperature. Dielectric studies have been carried out on these samples by using a HP 4192A LF impedance analyser from 5 kHz to 13 MHz. The real and imaginary parts of the dielectric constant were computed according to Polder [7].

Microstructural studies such as grain size and pore distribution were made by using a Jeol model T330A scanning electron microscope. Chemical analysis and atomic absorption spectrometry of the samples have been made to estimate Fe^{2+} concentration present in and zinc lost from each sample.

3. Results and discussion

3.1. Resistivity measurements

3.1.1. Results

Variations of room temperature (RT) resistivity ρ for the composition $Ni_{0.65}Zn_{0.35}Fe_2O_4$ as a function of sintering temperature (for fixed sintering times) and sintering time (for fixed sintering temperatures) are shown in Fig. 1a and b. The resistivity, as a function of sintering temperature, is observed to decrease gradually up to a sintering temperature of 1250 °C and thereafter the decrease is observed to be rapid. The decrease in ρ with time of sintering is also gradual and less rapid for the samples sintered at temperatures 1150 and 1200 °C, whereas it decreases rapidly with the increase in sintering time for the samples sintered at 1250 °C. The samples sintered at 1300 °C for various sintering times showed the lowest values of resistivity. It can be concluded from the above that the value of ρ begins to undergo a drastic change at the firing schedule of 1250 °C/2 h.

The resistivity dependence on temperature was studied in the range from room temperature to the Curie temperature. For some samples, the range was extended to a few degrees beyond the Curie temperature. Typical plots of log ρ versus $1000/T$ for the samples sintered at 1200 °C for 1 h and 1300 °C for 4 h are shown in Fig. 2a and b, respectively. The resistivity is observed to decrease exponentially with raising temperatue. The curves are almost linear at low temperatures, then a gradual change of slope occurs and finally they are once again found to be linear at high temperatures in all the cases. The temperature at which a cross-over point exists, due to the extension of tangents of the two linear

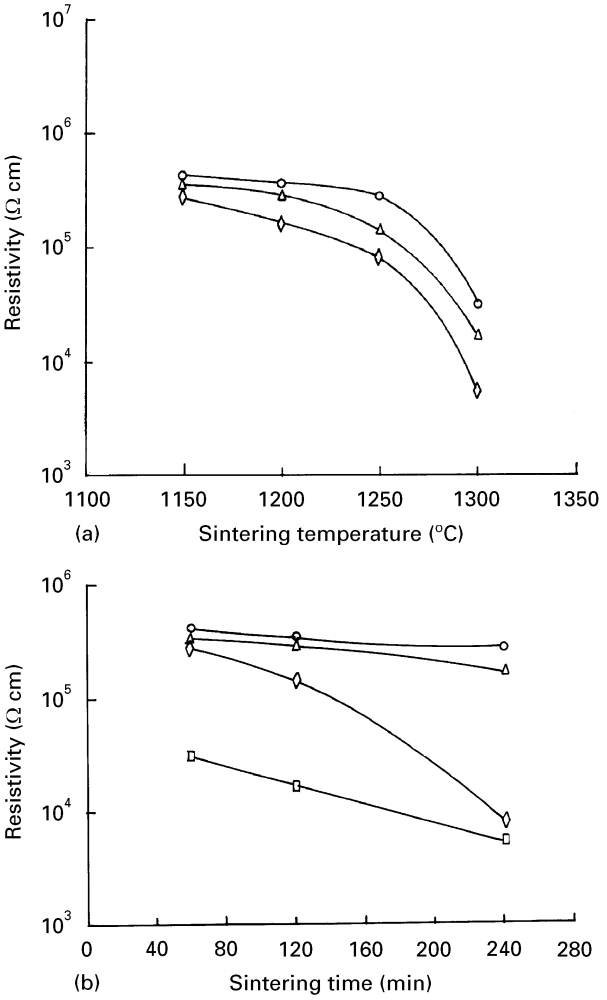

Figure 1 (a) Variation of resistivity of $Ni_{0.65}Zn_{0.35}Fe_2O_4$ with sintering temperature for various sintering times. (○) 1 h; (△) 2 h; (◇) 4 h. (b) Variation of resistivity of $Ni_{0.65}Zn_{0.35}Fe_2O_4$ with sintering time for various sintering temperatures (○) 1150 °C; (△) 1200 °C; (◇) 1250 °C; (□) 1300 °C.

regions, has no correlation with the observed Curie temperature.

Activation energies (E_1 and E_2) corresponding to the two regions (T_1 and T_2) for each sample have been estimated and are listed in Table I. The variation of resistivity as a function of applied field in all the cases has also been measured. The resistivity has been observed to decrease with the increase in the d.c. electric field.

3.1.2. Discussion

3.1.2.1. Resistivity and its dependence on sintering conditions. The observed variations in RT resistivity can be explained on the basis of microstructural changes brought about by the changes in sintering conditions. The values of RT resistivity along with the values of density, average grain diameter (D), Fe^{2+} concentration and zinc loss for various samples sintered at different temperatures for 4 h are listed in Table II. The values of density, grain diameter and wt % of Fe^{2+} concentration are found to increase with increase of firing temperature. Verwey and de Boer [8] have established that in oxides, containing ions of a given element present in more than one valence

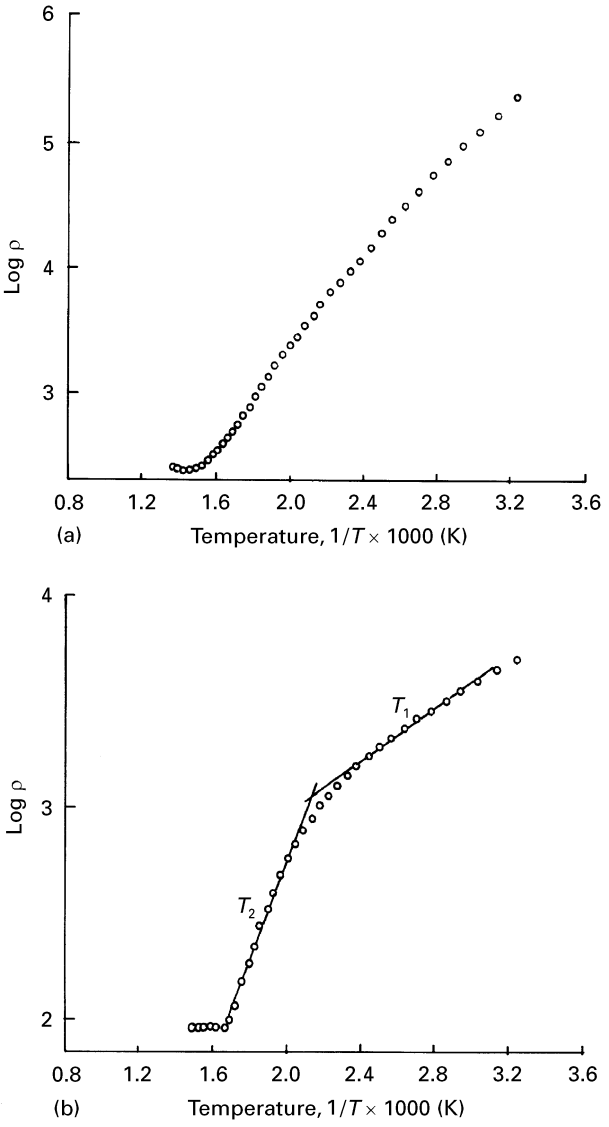

Figure 2 (a) Typical curve of log ρ versus $1000/T$ in the range 300 to 700 K of $Ni_{0.65}Zn_{0.35}Fe_2O_4$sintered at 1200 °C for 1 h. (b) Typical curve of log ρ versus $1000/T$ in the range 300 to 700 K of $Ni_{0.65}Zn_{0.35}Fe_2O_4$ sintered at 1300 °C for 4 h.

state, conduction takes place through hopping of electrons between trivalent and divalent iron ions within the octahedral positions without causing a change in the energy state of a crystal as a result of the transitions. Obviously, the more the divalent iron content the higher the conduction and consequently a decrease in the resistivity. Therefore, the observed decrease in RT resistivity with the increase of sintering temperature has been attributed to the presence of increased divalent iron content. Further, the increasing values of density and average grain diameter with increasing firing temperature also contribute to lower the resistivity by the following: (i) decreasing the activation energies [9]; (ii) increasing the effective area of grain to grain contact [3]; and (iii) decreasing the effective area of grain boundaries. Decreased porosity causes individual grains to come close, while the increased average grain diameter reduces the grain boundary dimensions; both invariably increase the cross-sectional area of the conductor, thus causing a decrease in the total resistance of the matrix [3]. The observed variations in resistivity with respect to sintering conditions are in accordance with the above considerations.

Nevertheless, from the observed data, it can be concluded that the volatilization of zinc is minimal upto a firing schedule of 1250 °C/2 h, and any increase thereafter either in sintering temperature or in sintering time causes more zinc to volatilize from the material, which in turn increases the presence of Fe^{2+} content, thus causing a decrease in the resistivity.

3.1.2.2. Resistivity and its dependence on temperature. The plots of log ρ versus $1000/T$ exhibit semiconductor behaviour in all the materials. In some of the samples for which studies were condcuted up to the Curie temperature, the plots showed two regions or one break, whereas in others for which the studied temperature range was extended to a few degrees beyond the Curie temperature, the plots showed three regions, i.e. two breaks. In this latter case, the second break occurs in the neighbourhood of the Curie temperature and this has been attributed to the influence of magnetic ordering over the conduction mechanism [10]. Whereas in the case of first/single break i.e. the observed change of slope at around 200 °C, which is consistent with all the samples, a similar explanation as was given by Rosenberg and Velicescu [11] in the case of cobalt containing mixed ferrites suits to explain the existing trend. For the low temperature process (T_1 region) the dominant conduction mechanism is thought to be an electron exchange between nearest neighbour $Fe^{2+} \Leftrightarrow Fe^{3+}$ pairs for which the associated activation energies are of the order of 0.1 eV [12], whereas for the high-temperature process (T_2 region) the migration is expected via Ni^{2+} or Fe^{3+} neighbours, i.e.

$$Ni^{2+} + Fe^{3+} \Leftrightarrow Fe^{2+} + Ni^{3+}$$

TABLE I Activation energies E_1 and E_2 corresponding to low and high temperature regions T_1 and T_2 of $Ni_{0.65}Zn_{0.35}Fe_2O_4$ with respect to various sintering conditions

Sintering temperature (°C)	Sintering time = 1 h		Sintering time = 2 h		Sintering time = 4 h	
	E_1 (eV)	E_2 (eV)	E_1 (eV)	E_2 (eV)	E_1 (eV)	E_2 (eV)
1150	0.39	0.40	0.36	0.44	0.25	0.54
1200	0.32	0.42	0.32	0.43	0.30	0.46
1250	0.32	0.39	0.32	0.42	0.29	0.44
1300	0.25	0.47	0.14	0.60	0.13	0.37

TABLE II Resistivity and other parameters of $Ni_{0.65}Zn_{0.35}Fe_2O_4$ sintered at various temperatures for 4 h

Sintering temperature (°C)	$\rho \times 10^4$ (Ω cm)	Density ($g\,cm^{-3}$)	Grain size (μm)	Fe^{2+} concentration (wt%)	Zinc loss (wt%)
1150	27.50	4.78	2.56	0.245	3.20
1200	16.40	4.80	3.55	0.367	4.50
1250	8.10	4.82	4.45	0.564	10.1
1300	0.55	4.84	5.70	0.971	16.6

The activation energy would then be higher and its value would be expected to depend on the concentration of the Ni^{3+} or Fe^{2+} ions. The observed values of activation energy for the two regions for all the samples (listed in Table I) are in conformity with the above considerations. The observed breaks in the vicinity of 200 °C appears increasingly prominent with the increase in sintering temperature. This is because concentration of Fe^{2+} ions in these samples causing more diffusion of electrons and thus leads to a reduction in activation energy values of the low-temperature region. Observations similar to the present study, i.e. the appearance of two or more breaks in the log ρ versus $1000/T$ curves, have also been reported in many cases [13, 14].

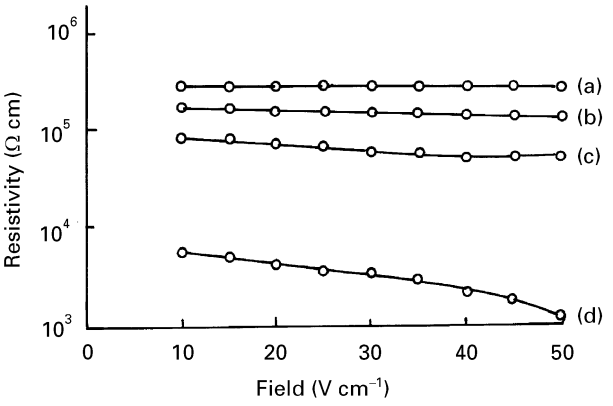

Figure 3 Variation of resistivity of $Ni_{0.65}Zn_{0.35}Fe_2O_4$ as a function of applied field for a sintering time of 4 h at various sintering tempertures. (a) 1150 °C; (b) 1200 °C; (c) 1250 °C; (d) 1300 °C.

3.1.2.3. Resistivity and its dependence on applied d.c. field. Typical variations of resistivity as a function of applied field for some samples are shown in Fig. 3. The resistivity was observed to decrease with the increase of field. This can be explained on the basis of Heywang's model [15] by assuming that the resistivity of the material is a sum of the contributions due to grains and grain boundaries. According to Heywang [16], there exists a localized state in the forbidden gap which corresponds to the surface states at the boundary. These surface states are due to surface imperfections and impurities at the surface. In the absence of any external field, some of these states are occupied by electrons resulting in a space charge region which generates potential barrier on either side of the boundary. On application of the electric field the Fermi level shifts and also the potential barriers are modified due to the increase in electron concentration and decrease in hole concentration at the boundary. This decreases the grain boundary resistance of the sample with the increase in applied voltage.

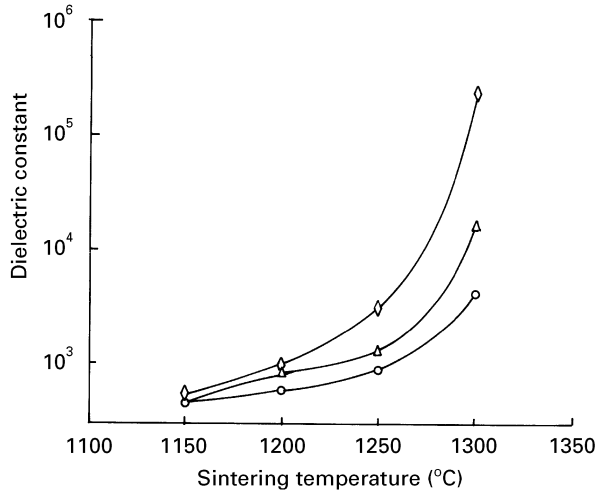

Figure 4 Variation of dielectric constant of $Ni_{0.65}Zn_{0.35}Fe_2O_4$ with sintering temperature for various sintering times. (○) 1 h; (△) 2 h; (◇) 4 h.

3.2. Dielectric properties

3.2.1. Results

The variations in dielectric constant with respect to various sintering conditions are presented in Fig. 4. The values of dielectric constant are found to increase with increase of sintering temperature or sintering time. The behaviour is opposite in comparison to variations in resistivity with sintering conditions. The frequency response of dielectric constant of Ni–Zn ferrites was also studied and a typical plot of dielectric constant versus frequency in the range 5 kHz to 10 MHz is shown in Fig. 5. Dispersion in dielectric constant was exhibited by all the samples in the studied frequency range. Dispersion is maximum for the sample sintered at 1300 °C for 4 hours and the magnitude of dispersion decreases continuously with the decrease of sintering temperature or sintering time. Dielectric relaxation intensity, i.e. the difference between low frequency dielectric constant and high frequency dielectric constant has been calculated and its variation with sintering temperature for various sintering times is plotted in Fig. 6. The variation showed a similar trend as that of low frequency dielectric constant versus sintering conditions. The variations of tan δ with frequency for different sintering conditions are shown in Fig. 7. The variation in all cases was observed to show a dispersion. Dielectric loss peaks

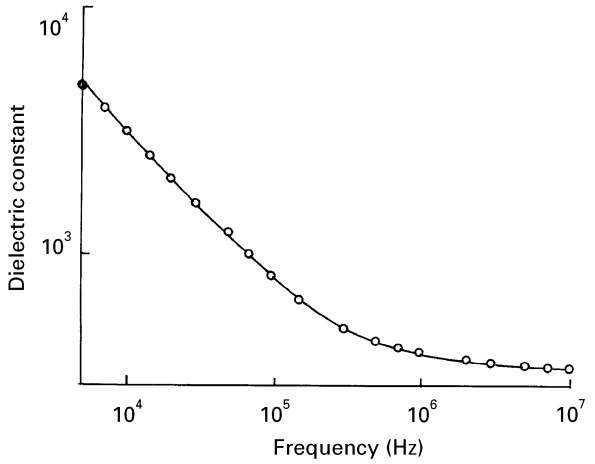

Figure 5 Typical curve showing frequency response of dielectric constant of $Ni_{0.65}Zn_{0.35}Fe_2O_4$ sintered at 1250 °C for 4 h.

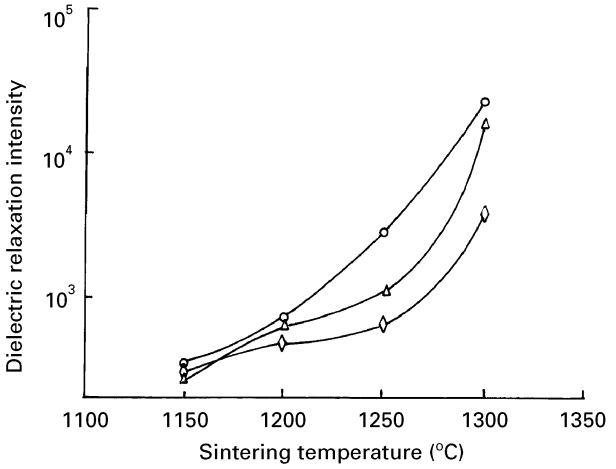

Figure 6 Variation of dielectric relaxation intensity of $Ni_{0.65}Zn_{0.35}Fe_2O_4$ with sintering temperature for various sintering times. (○) 1 h; (△) 2 h; (◇) 4 h.

were observed for a few samples which exhibit low resistivities.

3.2.2. Discussion

3.2.2.1. Dielectric constant and its dependence on sintering conditions. The observed dielectric behaviour can be explained on the basis of the assumption [17] that the mechanism of dielectic polarization is similar to that of conduction and the electronic exchange such as $Fe^{2+} \Leftrightarrow Fe^{3+}$ results in a local displacement of the electrons in the direction of electric field which determines the polarization of the ferrites. As discussed earlier, the increase of sintering temperature has brought about an increase in the Fe^{2+} concentration and is, therefore, responsible for the increase in polarization. Thus, a comparatively high value of dielectric constant is expected for the sample sintered at 1300 °C for 4 h, because the number of Fe^{2+} ions available for polarization is maximal for this sample. Any decrease thereafter either in the sintering temperature or in the sintering time only decreases the available Fe^{2+} concentration and causes a decrease in the dielectric constant. Further, the increase in grain size (Table I) with

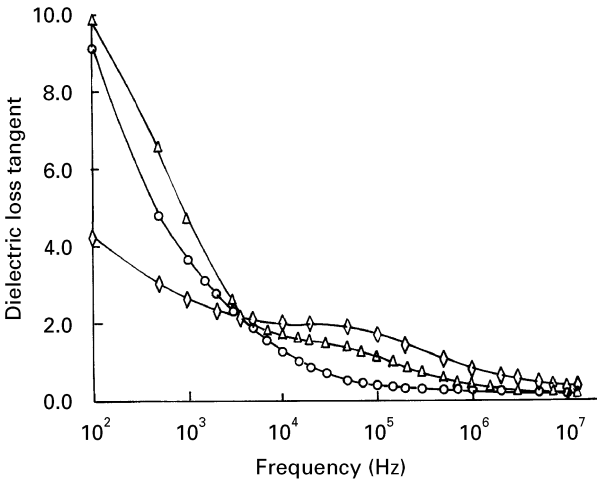

Figure 7 Typical curves of $Ni_{0.65}Zn_{0.35}Fe_2O_4$ showing frequency response of dielectric loss tangent for various sintering conditions. (○) 1150 °C, 2 h; (△) 1250 °C, 2 h; (◇) 300 °C, 1 h.

the increase of sintering temperature causes an increase in the grain to grain boundary thickness ratio [18] which is also responsible for the increase in dielectric constant [19]. The observed values of dielectric constant with respect to sintering conditions are in accordance with the above considerations.

3.2.2.2. Frequency dependence of the dielectric constant. Dielectric dispersion in ferrites can be explained on the basis of space change polarization which is a result of the presence of higher conductivity phases (grains) in the insulating matrix (grain boundaries) of a dielectric causing localized accumulation of charge under the influence of an electric field [20]. Since an assembly of space charge carriers in a dielectric requires finite time to line up their axes parallel to an alternating electric field, if the frequency of the field reversal increases, a point will be reached when the space charge carriers can not keep up with the field and the alternation of their direction lags behind that of the field [20]; thus resulting in a reduction in the dielectric constant of the material. As the frequency of the field continues to increase, at some stage the space charge carriers will barely have started to move before the field reverses and make virtually no contribution to the polarization of the dielectric.

Because the alternation of space charge polarization requires a whole body of charge to be moved through a resistive material, the dielectric dispersion is dependent on the number of available space charge carriers as well as the resistivity of the material. As is evident from Fig. 1a, the resistivity has been observed to decrease with the increase in sintering temperature. This is responsible for pile up of more charge at the layer interface and increases the space charge polarization as well as the dielectric intensity with the increase of sintering temperature. The variations in dielectric relaxation intensity as a function of sintering temperature are in agreement with the above considerations.

3.2.2.3. Frequency dependence of dielectric loss tangent. The dielectric loss tangent in each sample is found to decrease with the increase in frequency. In some samples which possess considerable Fe^{2+} content and exhibiting low resistivities, the frequency response of the dielectric loss tangent is found to be slightly different from the above by resulting apparently upward kinks around the frequency of 100 kHz. The small increases and subsequent decreases with frequency in dielectric loss tangent in these samples sintered at 1250 °C/2 h and 1300 °C/1 h as shown in Fig. 7 may be attributed to dielectric loss peaks. However, confirmations of this extent require more experimental data, probably at different temperatures.

The occurrence of peaks in $\tan\delta$ versus frequency curves can be explained qualitatively. Iwauchi [22] pointed out that there is a strong correlation between the conduction mechanism and dielectric behaviour. The conduction in these ferrites is considered as due to the hopping of electrons between divalent and trivalent iron ions over the octahedral sites. A peak in the dielectric loss tangent ($\tan\delta$) is observed when this hopping frequency is approximately equal to the frequency of the external applied electric field [23].

References

1. L. G. VAN UITERT, *J. Chem. Phys.* **23** (1955) 1883.
2. D. R. SECRIST and H. L. TURK, *J. Amer. Ceram. Soc.* **53** (1970) 683.
3. A. B. NAIK and J. I. POWAR, *Ind. J. Pure & Appl. Phys.* **23** (1985) 436.
4. G. C. JAIN, B. K. DAS, R. B. TRIPATHI and RAM NARAYAN, *IEEE Trans. Magn.* **MAG-18** (1982) 776.
5. C. G. KOOPS, *Phys. Rev.* **83** (1951) 121.
6. G. F. DIONNE and R. G. WEST, *J. Appl. Phys.* **61** (1987) 3868.
7. D. POLDER, *Proc. IEE* **97–II** (1950) 246.
8. E. J. W. VERWEY and J. H. DE BOER, *Rec. Trav. Chim. Pays-Bas.* **55** (1936) 531.
9. G. DIETZMANN, M. KROTZCH and S. WOLF, *Phys. Status Solidi* **2** (1962) 1762.
10. D. RAVINDER, PhD Thesis, Osmania Univesity, Hyderabad, India (1988).
11. M. ROSENBERG and M. VELICESCU, *J. Phys. Soc. Japan* **28** (1970) 264.
12. E. J. W. VERWEY and P. W. HAAYMAN, *Physica* **8** (1941) 1979.
13. B. V. BHISE, M. G. PATIL, M. B. DONGARE, S. R. SAWANT and S. A. PATIL, *Ind. J. Pure & Appl. Phys.* **30** (1992) 385.
14. S. A. PATIL, B. L. PATIL, S. R. SAWANT, A. S. JAMBHALE and R. N. PATIL, *ibid.* **31** (1993) 904.
15. W. HEYWANG, *J. Amer. Ceram. Soc.* **47** (1964) 484.
16. *Idem., Z. Angew. Phys.* **16** (1963) 1.
17. L. I. RABINKIN and Z. I. NOVIKOVA, "Ferrites" (Minsk, 1960) 146.
18. RAM NARAYAN, R. B. TRIPATHI and B. K. DAS, "Advances in ferrites", Vol. 1, edited by C. M. SRIVASTAVA and M. J. PATNI (Oxford & IBH Publishing Co., New Delhi, India, 1989) p. 267.
19. J. SMIT and H. P. J. WIJN, "Ferrites" (Philips Technical Library, 1959) p. 242.
20. MANAS CHANDA, "Science of engineering materials", Vol. 3 (The Macmillan Company of India Ltd., New Delhi, 1980) p. 103.
21. T. G. W. STIJNTJES, J. KLERK and A. B. V. GROENOU, *Philips. Res. Repts.* **25** (1970) 95.
22. K. IWAUCHI, *Jpn J. Appl. Phys.* **10** (1971) 1520.
23. V. R. K. MURTHY and J. SOBHANADRI, *Phys. Status Solidi* (*a*) **36** (1976) 133.
24. L. G. VAN UITERT, *Proc. IRE* **44** (1956) 1294.

Received 25 March 1996
and accepted 9 May 1997